Ultra-Peripheral Collisions (UPC) Jpsi Photoproduction

Wen-Chen Chang

September 18, 2025

References

- https://indico.cern.ch/event/1479384/contributions/6632169/attachments/3134241/5560712/sjdas_20250912_IS2025.pdf
- https://indico.cern.ch/event/1479384/contributions/6632167/attachments/3134178/5560709/Wenbin_Zhao_IS2025.pdf
- https://indico.ijclab.in2p3.fr/event/10641/contributions/35283/attachments/24301/35362/HadPhys30_2024.pdf
- https://inspirehep.net/literature/2825384
- https://inspirehep.net/literature/1802728
- https://journals.aps.org/prd/abstract/10.1103/PhysRevD.111.052006

Elastic J/ψ photoproduction

$$\gamma p \rightarrow J/\psi p$$

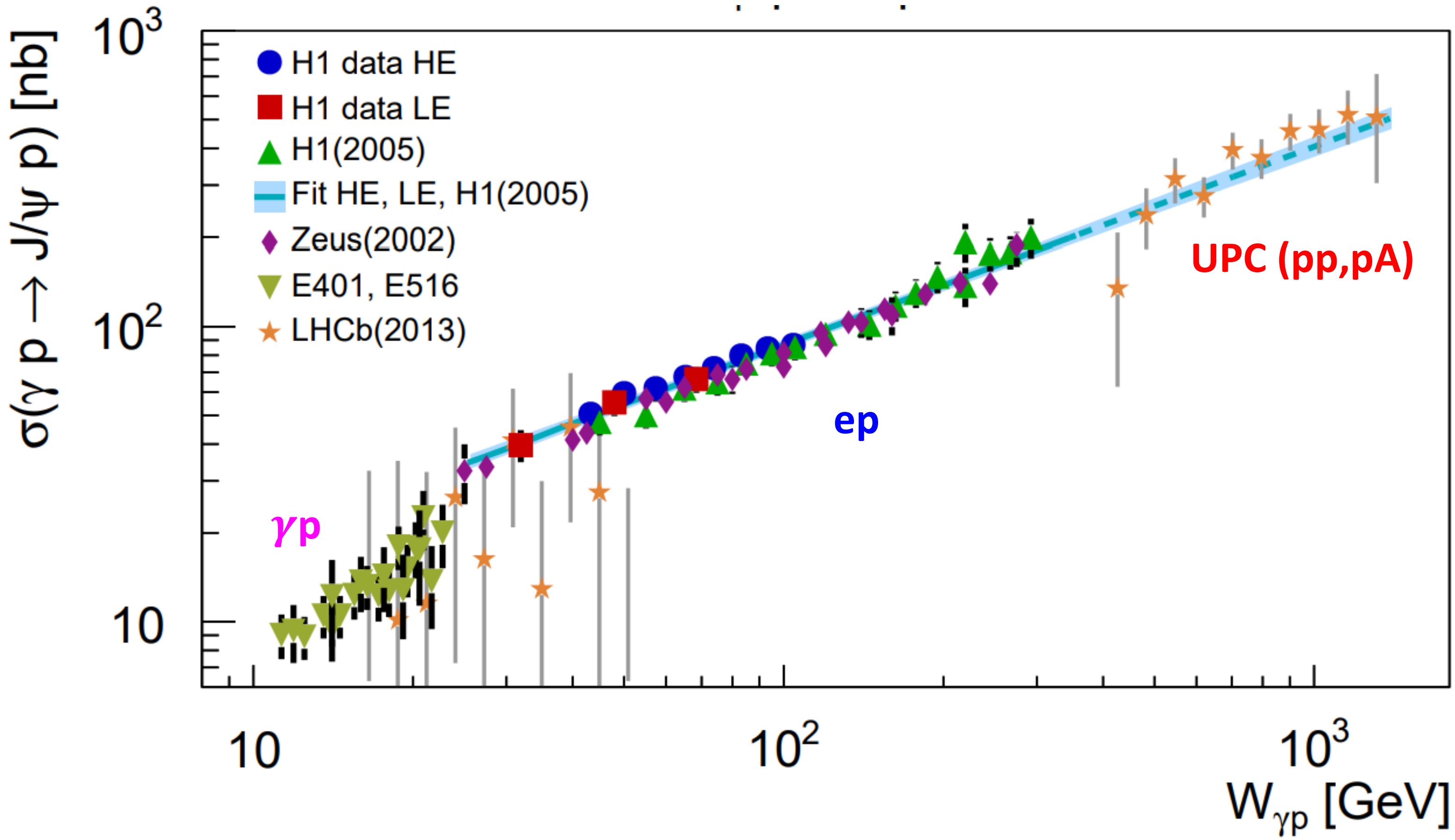

arXiv:1304.5162

Elastic J/ψ photoproduction

$$\gamma p \to J/\psi p$$

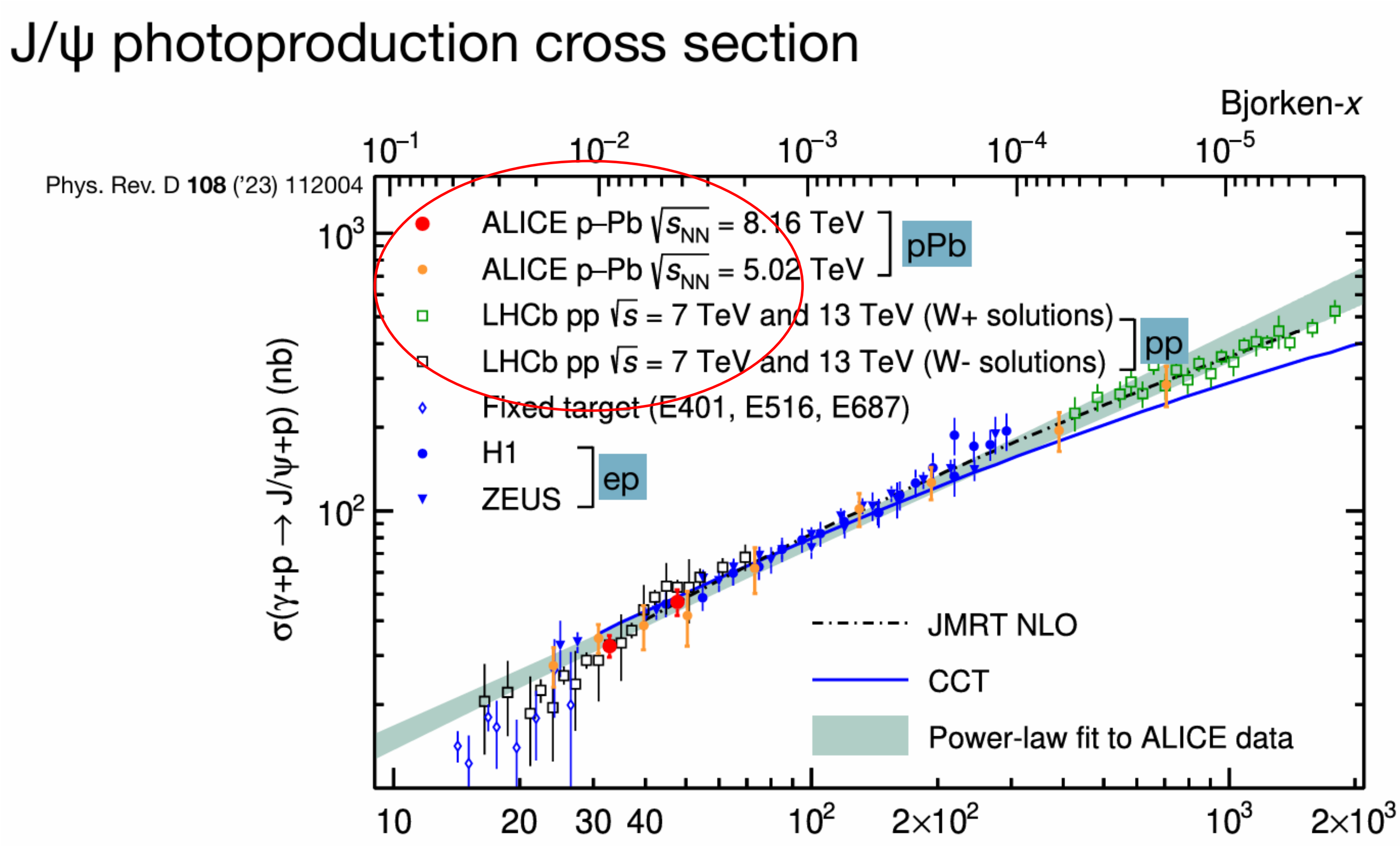

https://indico.ijclab.in2p3.fr/event/10641/contributions/35283/attachments/24301/35362/HadPhys30_2024.pdf

Elastic J/ψ photoproduction

$$\gamma p \rightarrow J/\psi p$$

Exclusive processes

Ultra-Peripheral Collisions (UPC)

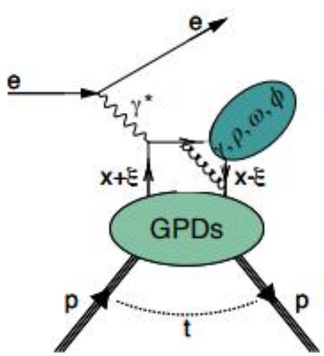

Hard exclusive meson production
Hard scale=large Q^2

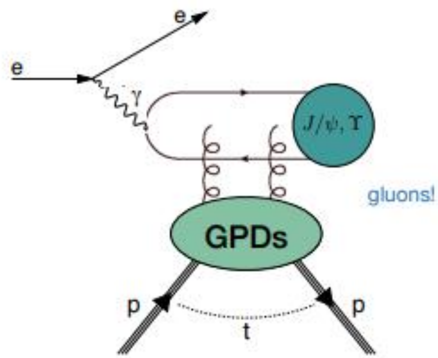

Exclusive meson photoproduction
Hard scale = large charm/bottom-quark mass

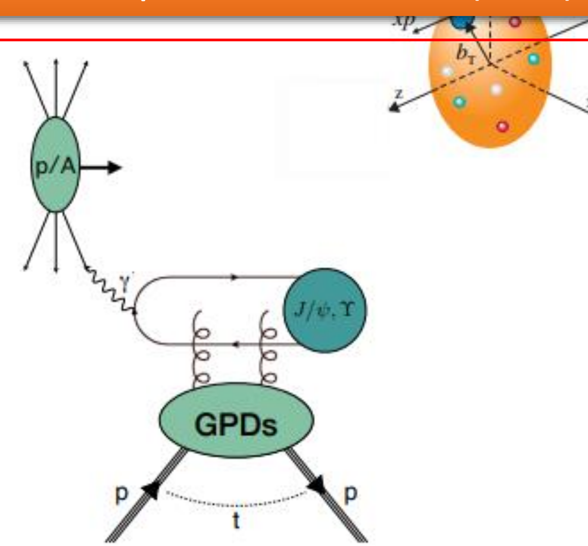

Exclusive meson photoproduction
Hard scale = large charm/bottom-quark mass

down to $x_B=10^{-4}$ at HERA/EIC in ep
$x_B=10^{-3}$ at EIC in eA

down to $x_B=10^{-6}$ at LHC in pp
$x_B=10^{-5}$ at LHC in pA

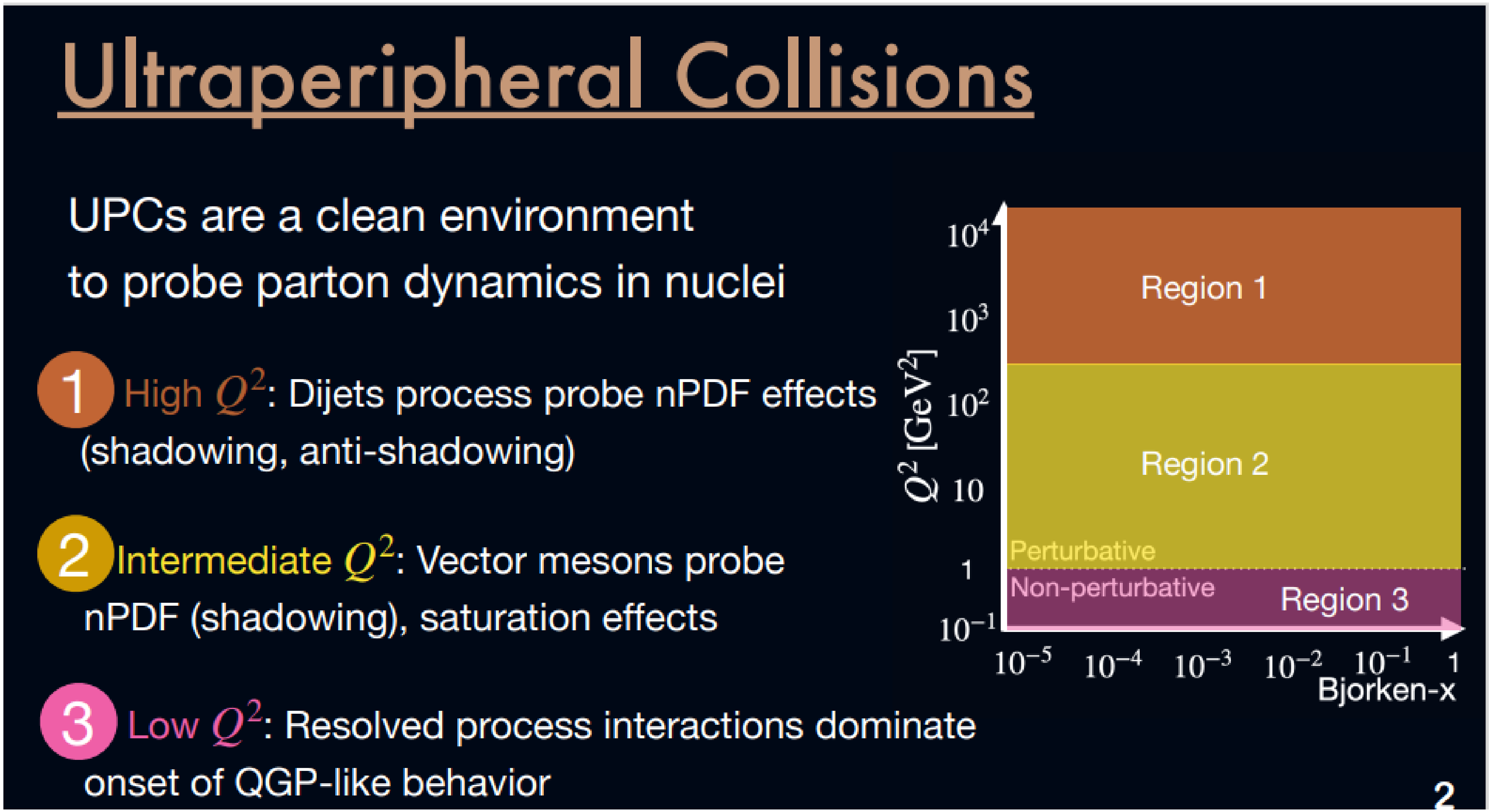

$$x = \frac{M_{probe}}{\sqrt{s}} e^{-y}$$

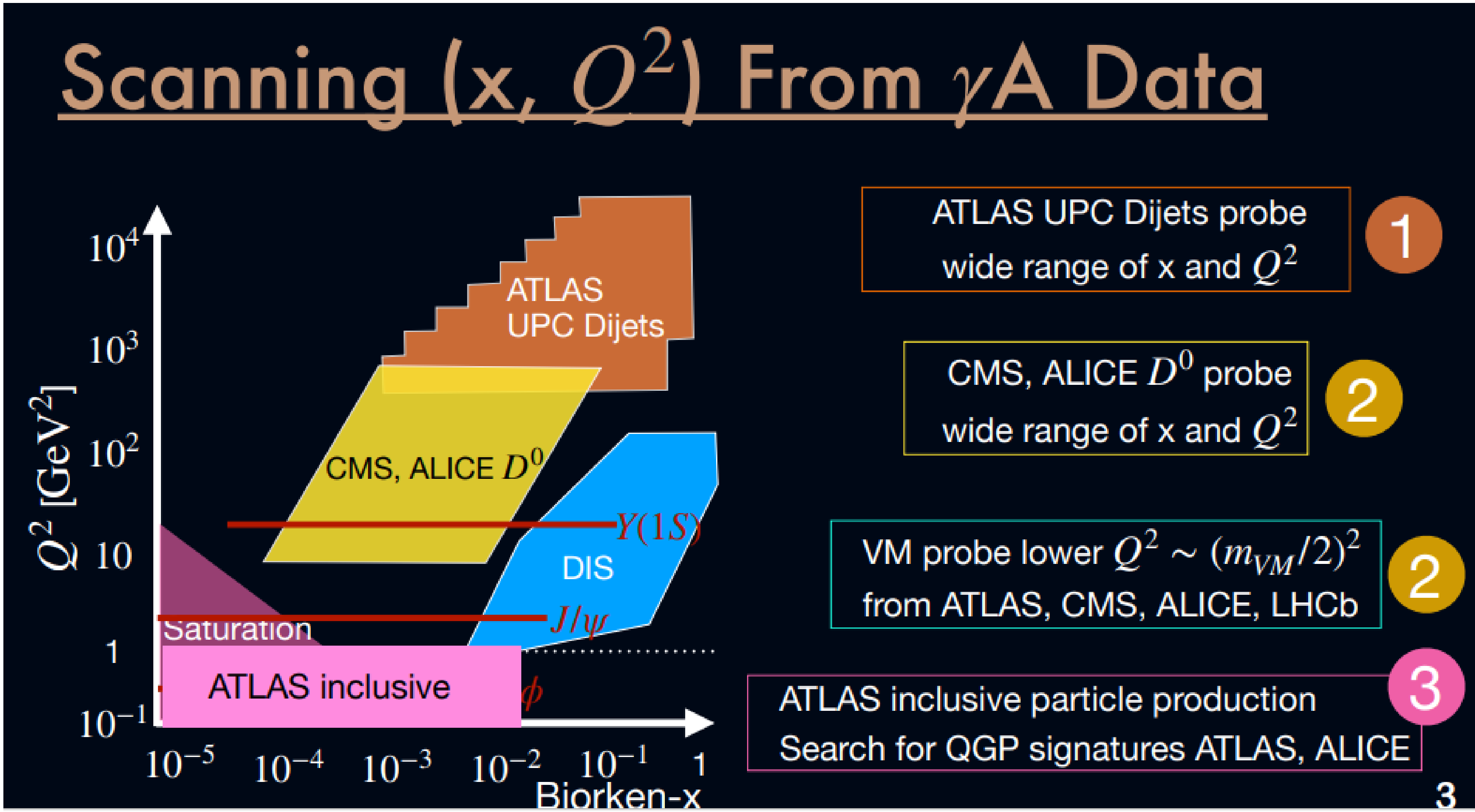

$$x = \frac{M_{probe}}{\sqrt{s}} e^{-y}$$

Identification of UPC events in ATLAS

- UPC photonuclear scattering can be distinguished from non-UPC hard-scattering processes by requiring the photon-emitting nucleus to remain intact. Experimentally, this is accomplished by using the zero-degree calorimeters (ZDCs), which detect the beam-energy neutrons emitted in most hadronic nuclear interactions. The condition that no neutrons (0n) are observed in one direction, combined with a requirement for gaps in the particle rapidity distribution on that side of the event, is effective at identifying photonuclear collisions.
- A requirement that at least one neutron (Xn) is observed in the other direction distinguishes photonuclear events from, for example, γγ scattering processes, and suppresses these backgrounds.
- Events of large rapidity gap.

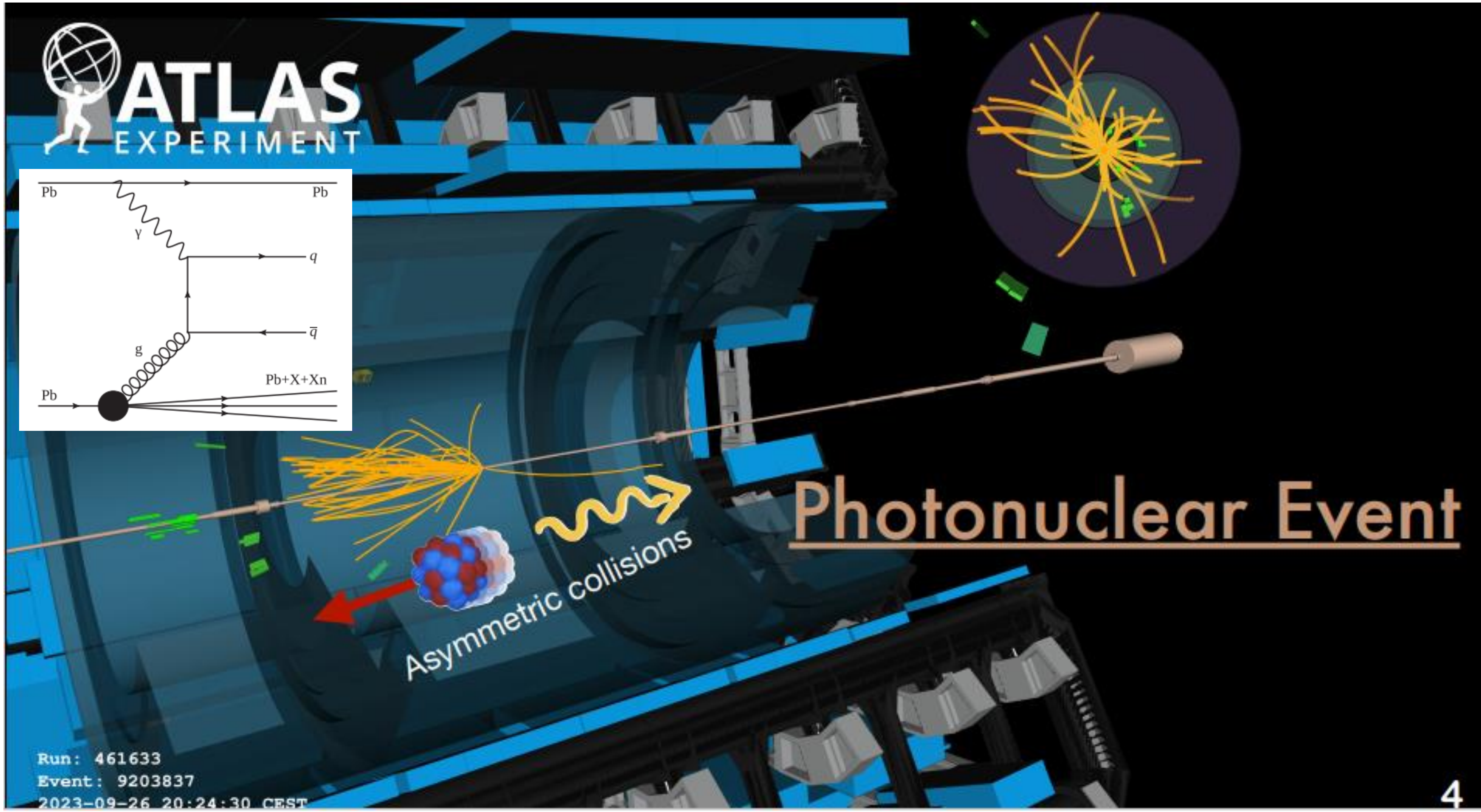

https://journals.aps.org/prd/abstract/10.1103/PhysRevD.111.052006

Trigger conditions: (a) 0nXn (b) ET (c) large-pT jet

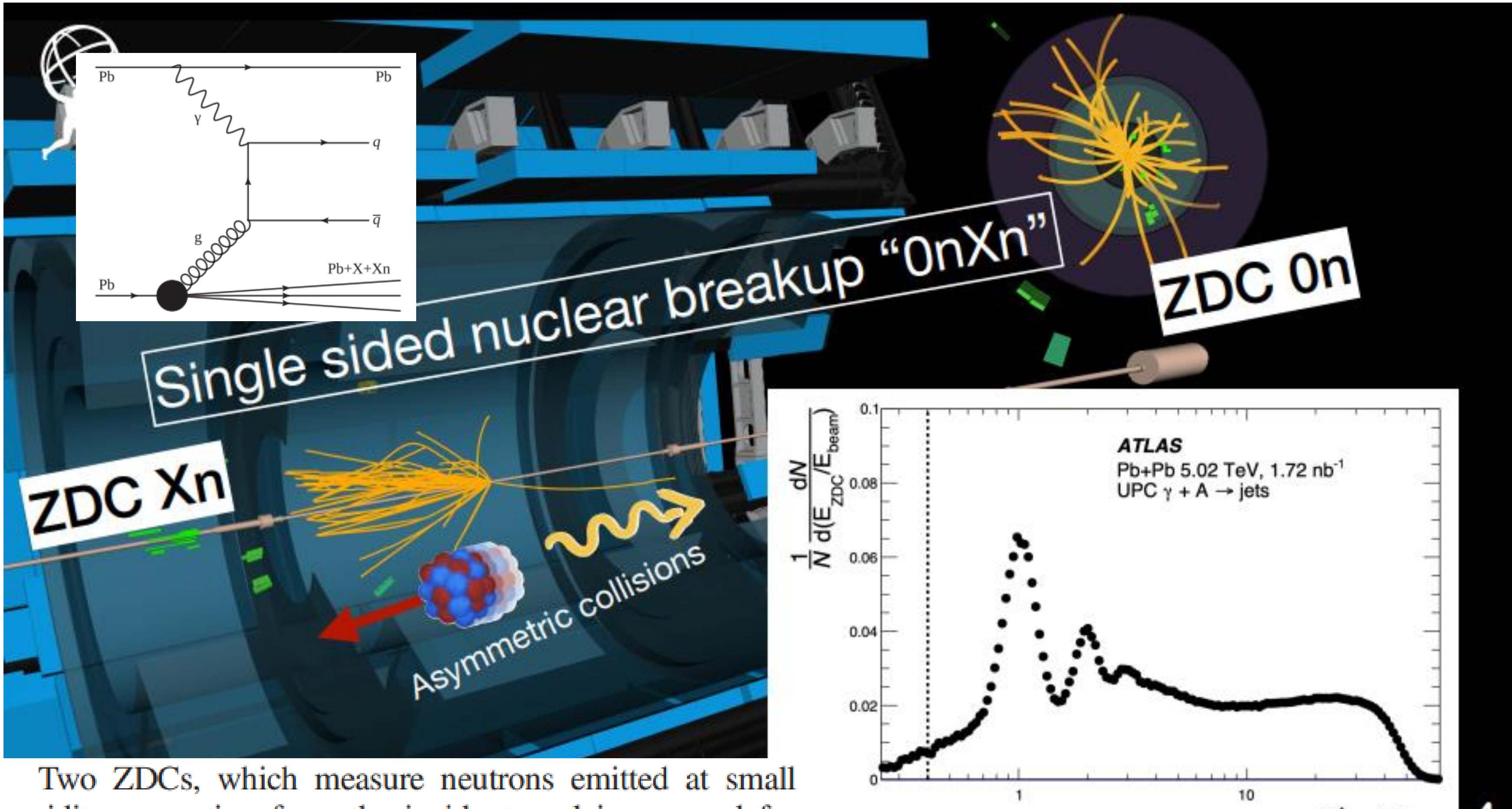

Two ZDCs, which measure neutrons emitted at small rapidity separation from the incident nuclei, are used for triggering and for offline event selection. The ZDCs are located symmetrically at a distance of ±140 m from the nominal IP and cover $|\eta| > 8.3$ along the beam axis. Each calorimeter consists of four modules, each containing slightly more than one interaction length of tungsten absorber.

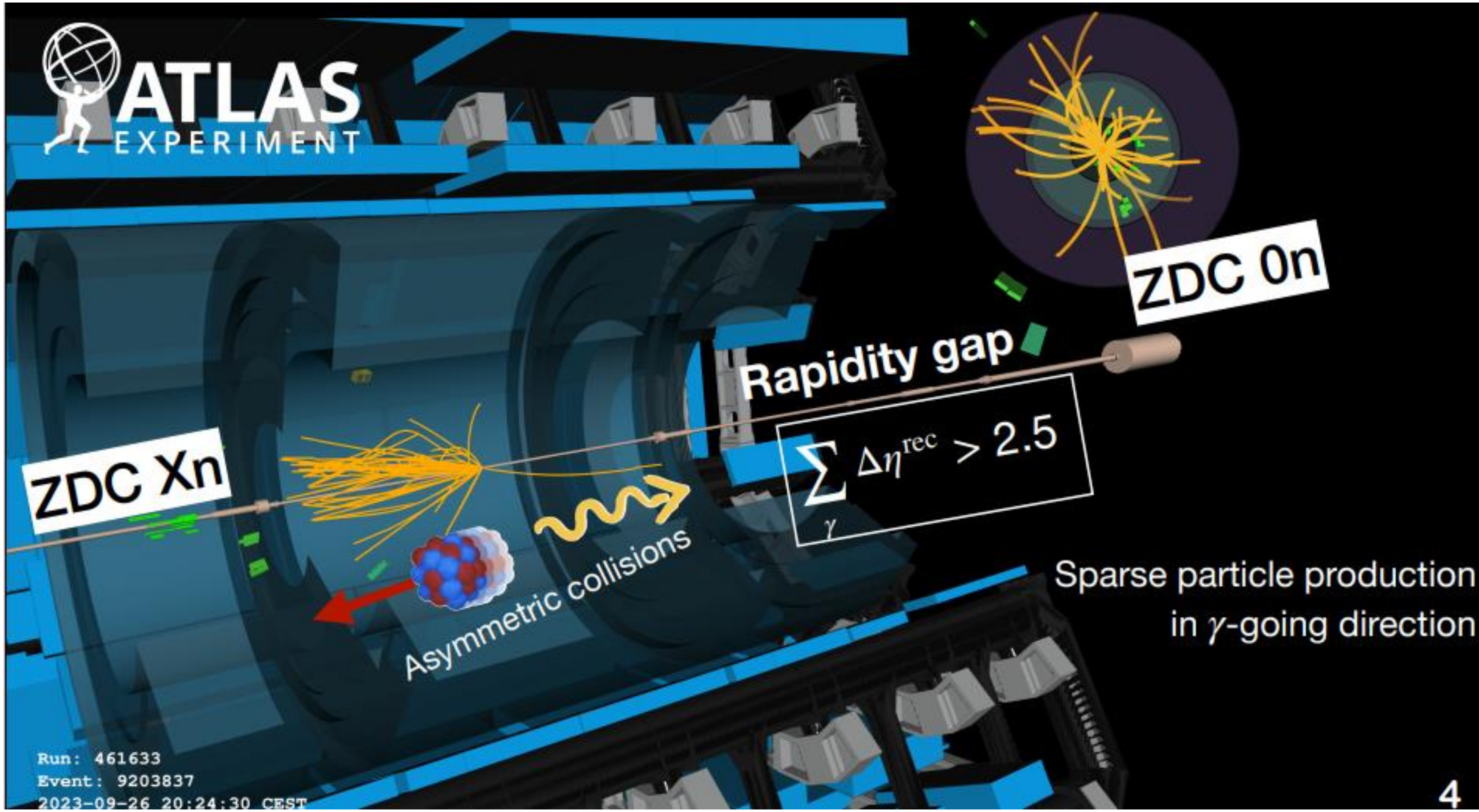

https://journals.aps.org/prd/abstract/10.1103/PhysRevD.111.052006

Large Rapidity Gap Events

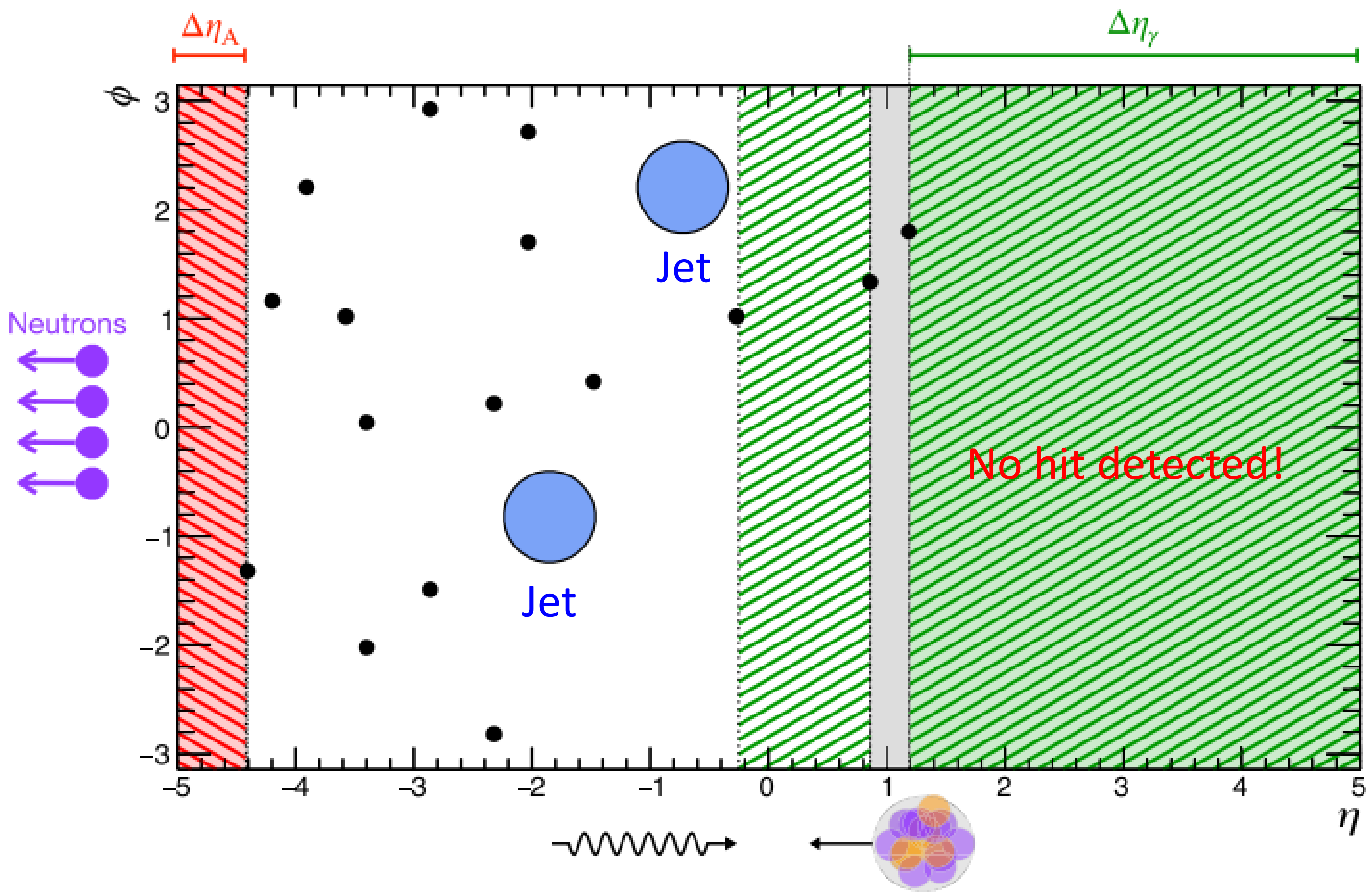

azimuthal angle around the z axis. The pseudorapidity is defined in terms of the polar angle θ as $\eta = -\ln\tan(\theta/2)$ and is equal to the rapidity $y = \frac{1}{2}\ln(\frac{E+p_z c}{E-p_z c})$ in the relativistic limit. Angular

Uncertainties of UPC

- Photon flux generated by a nucleus and a proton
- Photon energy, kinematics of DIS

$$H_T \equiv \sum_i p_{Ti}, \qquad (2)$$

while the N-jet system mass and rapidity are calculated as

$$m_{\text{jets}} \equiv \left[\left(\sum_i E_i \right)^2 - \left| \sum_i \vec{p}_i \right|^2 \right]^{1/2}, \qquad (3)$$

$$y_{\text{jets}} \equiv \frac{1}{2} \ln \left(\frac{\sum_i E_i + \sum_i p^*_{zi}}{\sum_i E_i - \sum_i p^*_{zi}} \right). \qquad (4)$$

$$z_\gamma \equiv \frac{m_{\text{jets}}}{\sqrt{s_{\text{NN}}}} e^{+y_{\text{jets}}},$$

Corresponding to y variable in DIS.

$$x_A \equiv \frac{m_{\text{jets}}}{\sqrt{s_{\text{NN}}}} e^{-y_{\text{jets}}},$$

https://inspirehep.net/literature/2825384

EUROPEAN ORGANIZATION FOR NUCLEAR RESEARCH (CERN)

CERN-EP-2024-213
LHCb-PAPER-2024-012
28 February 2025

Measurement of exclusive J/ψ and $\psi(2S)$ production at $\sqrt{s} = 13\,\text{TeV}$

LHCb collaboration†

LHCb: Exclusive Central Jpsi/psi' Production (pp -> p + J/psi + p)

Signal

Background

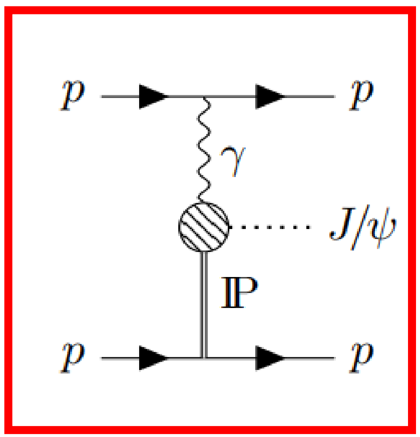

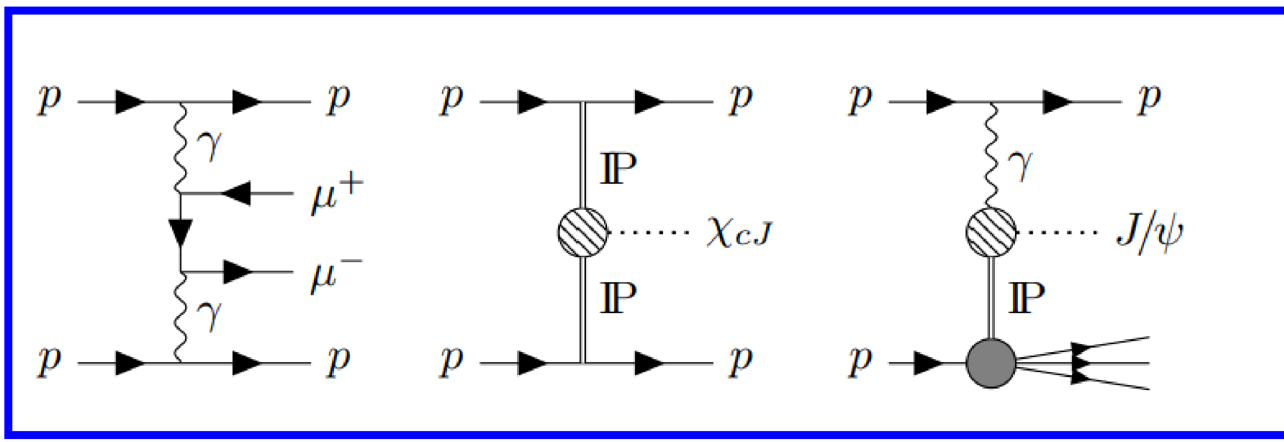

Central exclusive vector-meson production (CEP)

continuum dimuon production

chic via double Pomeron exchange

inelastic proton-dissociation (PD)

LHCb 2024

https://inspirehep.net/literature/2825384

LHCb Detector

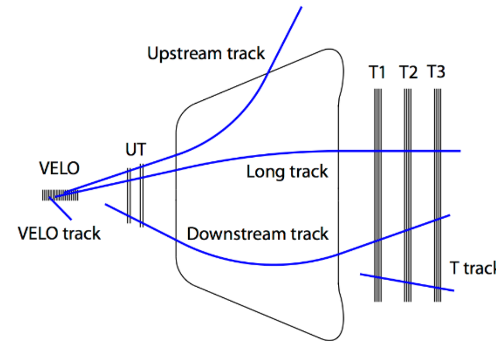

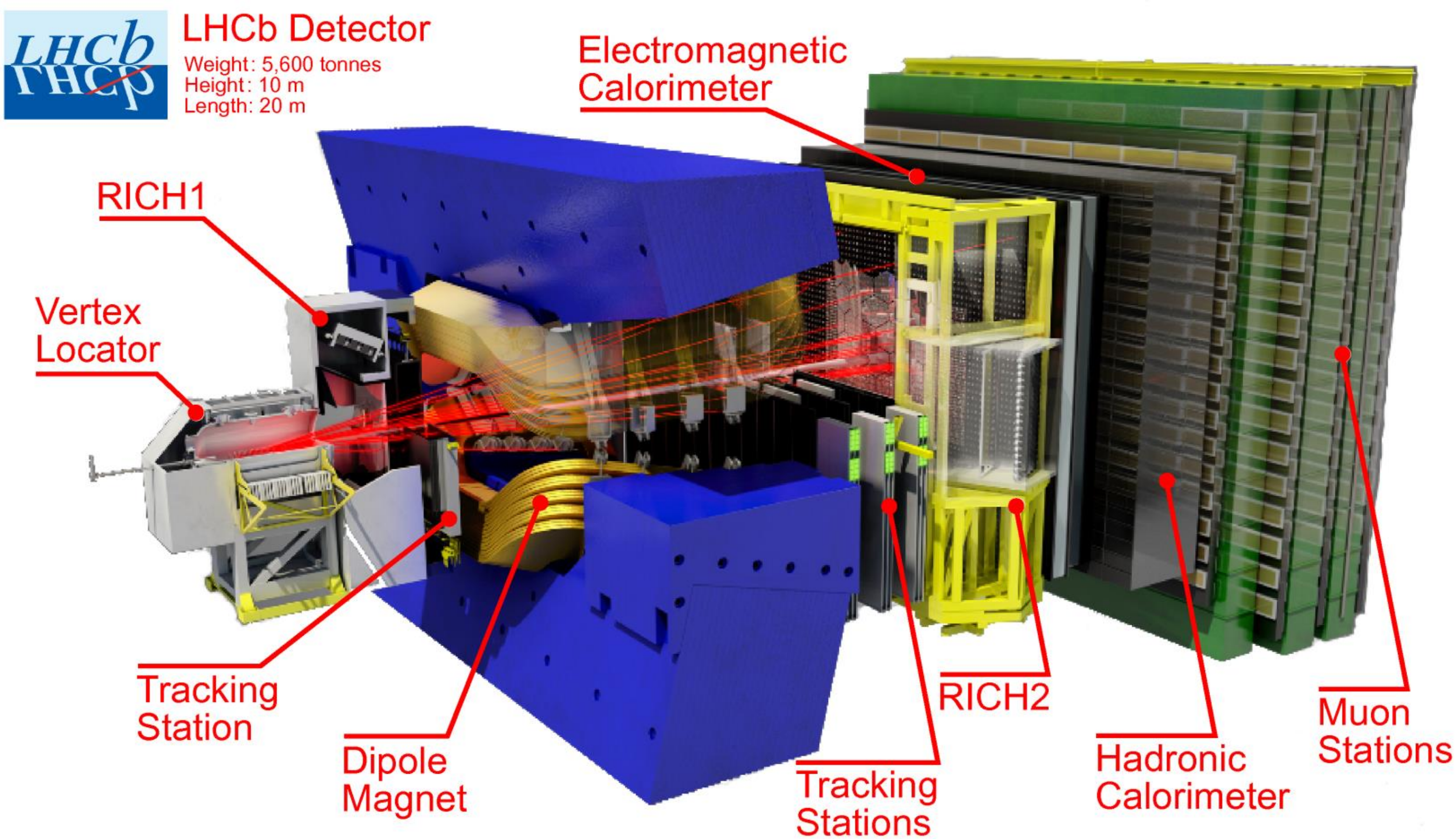

LHCb HERSCHEL detector: high-rapidity shower counters

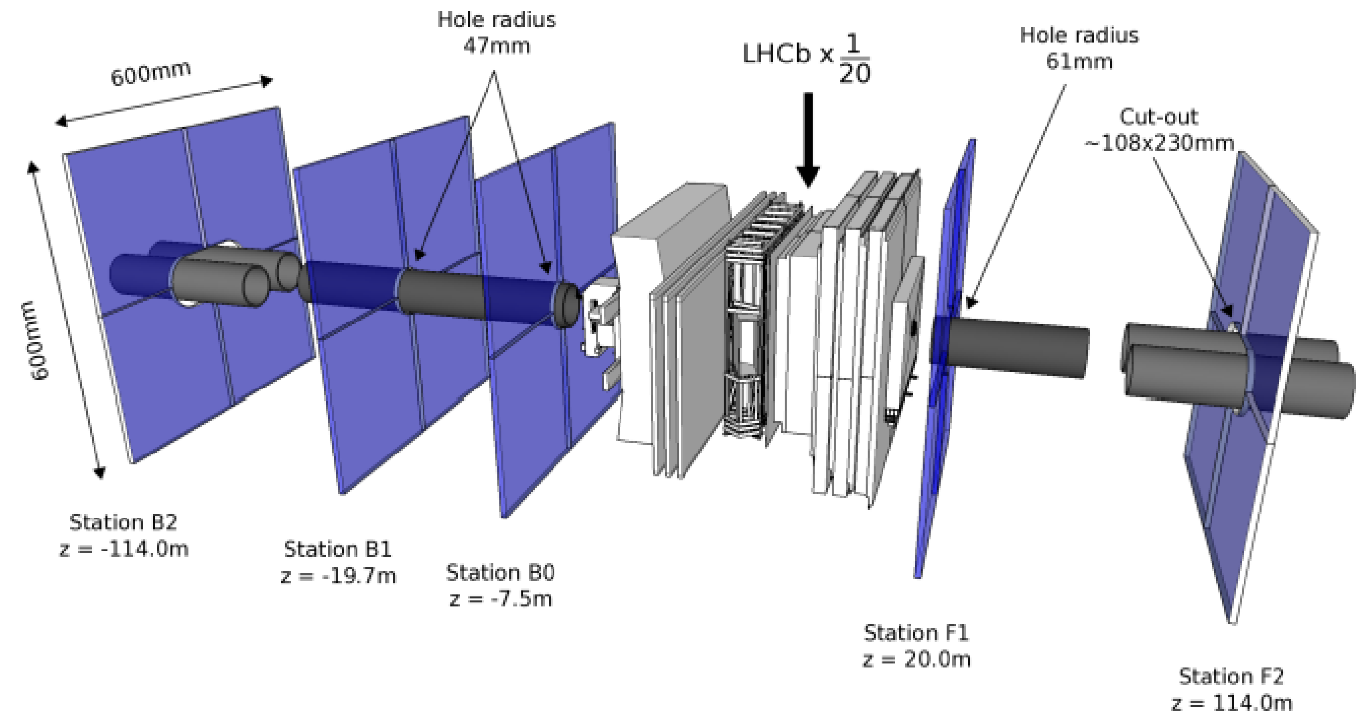

Figure 2. Layout of the active areas of the HeRSCheL stations around the LHCb interaction point (IP8), where for illustration the HeRSCheL stations have been magnified by a factor of 20 with respect to the rest of the LHCb detector. z-axis not to scale.

Event Selection

- Two muons with pT>400 MeV and p>3 GeV, fewer than 10 tracks in the VELO (large-area silicon-strip detector), -3.5<eta<-1.5 and 2<eta<5.
- No firing of HERSCHEL, -10<eta<-5 and 5<eta<10 (five planes of scintillators, as a veto).
- No photon other than those radiated from the muon.
- Control sample: a single muon with pT>400 MeV.

"Signal Sample" vs. "Control Sample"

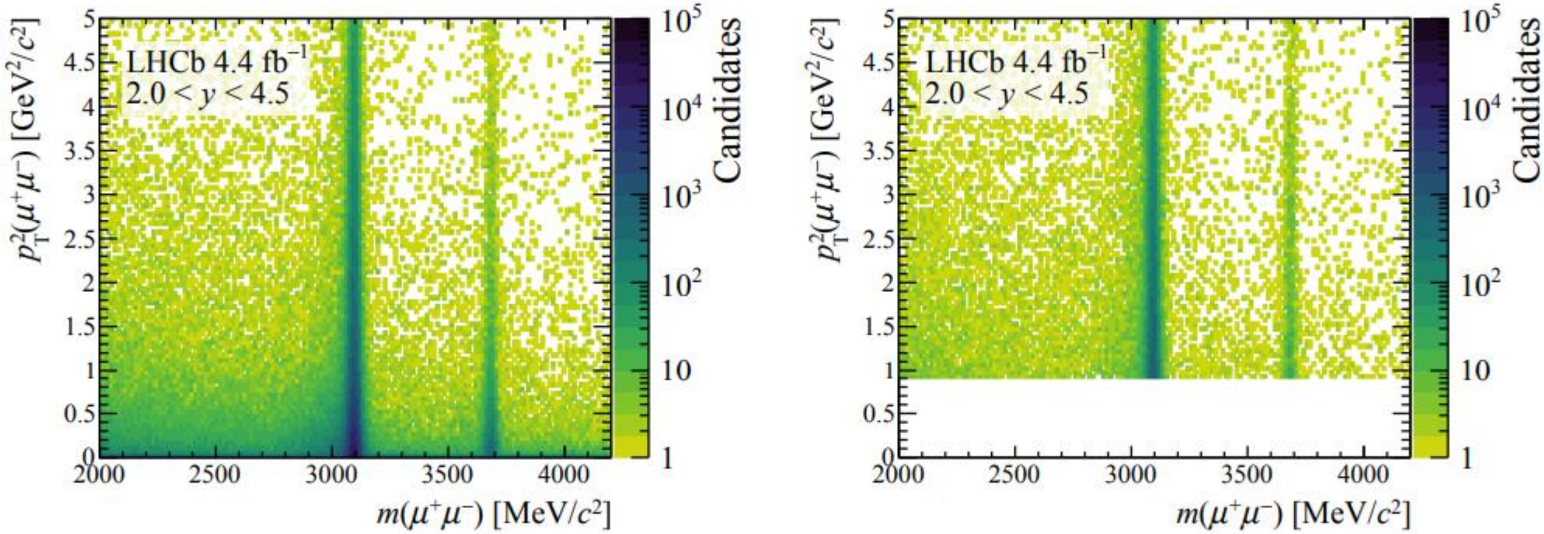

Figure 2: Two-dimensional mass-p_{T}^2 distributions for the (left) signal and (right) control samples.

Modeling of 2d distributions of [m, pT2] for Jpsi and psi'.

Fit in the “Control Sample”

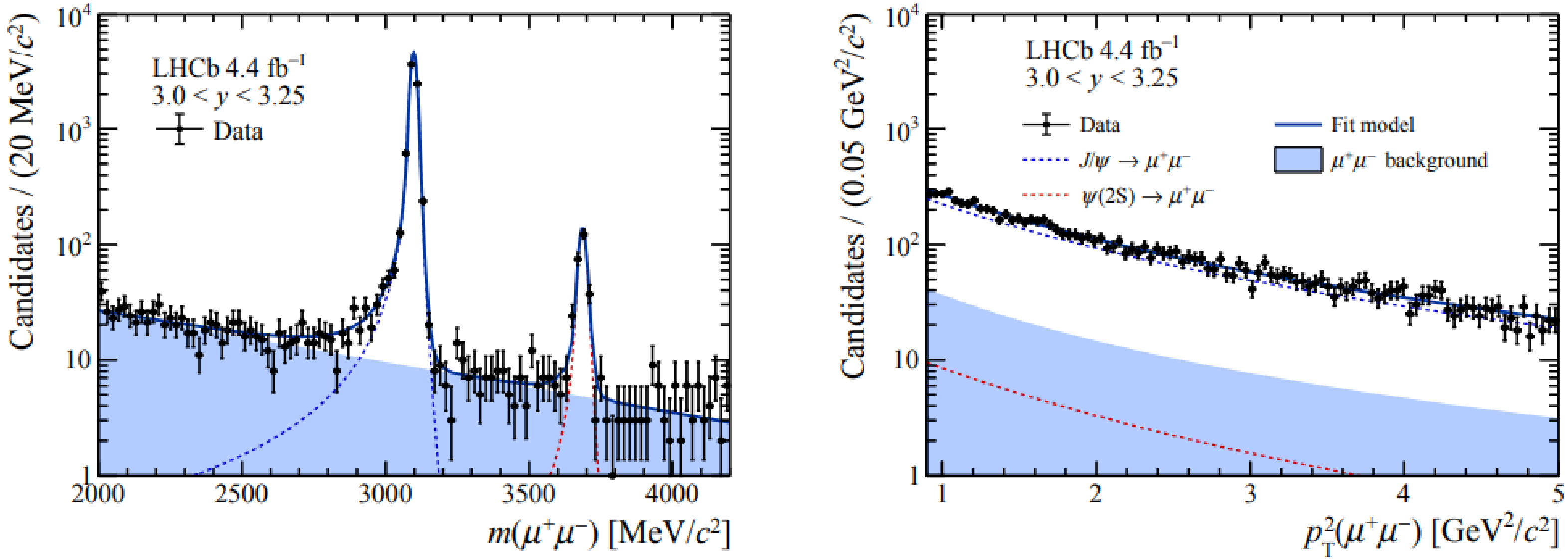

Modeling of 2d distributions of [m, pT2] for Jpsi and psi’.

Fit in the “Signal Sample”

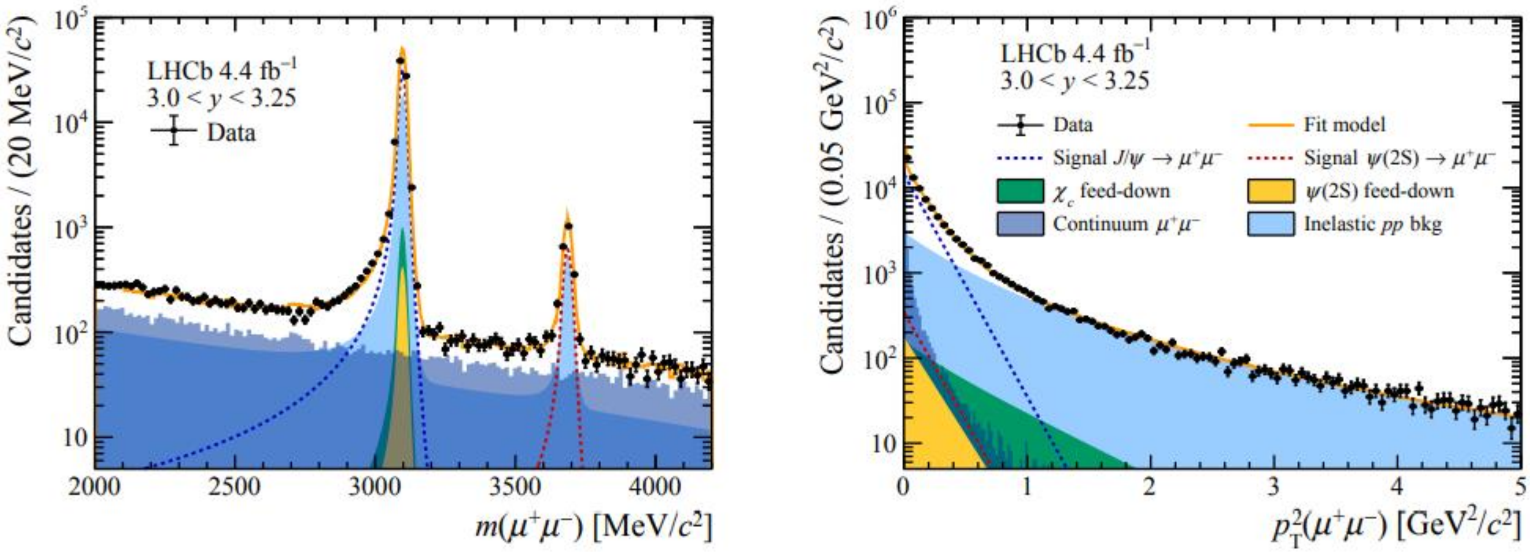

Figure 5: Distributions of (left) mass and (right) p_T^2 of data in the signal sample for the rapidity interval $3.0 < y < 3.25$. The fit described in the text is superimposed.

Fits in 10 rapidity bins

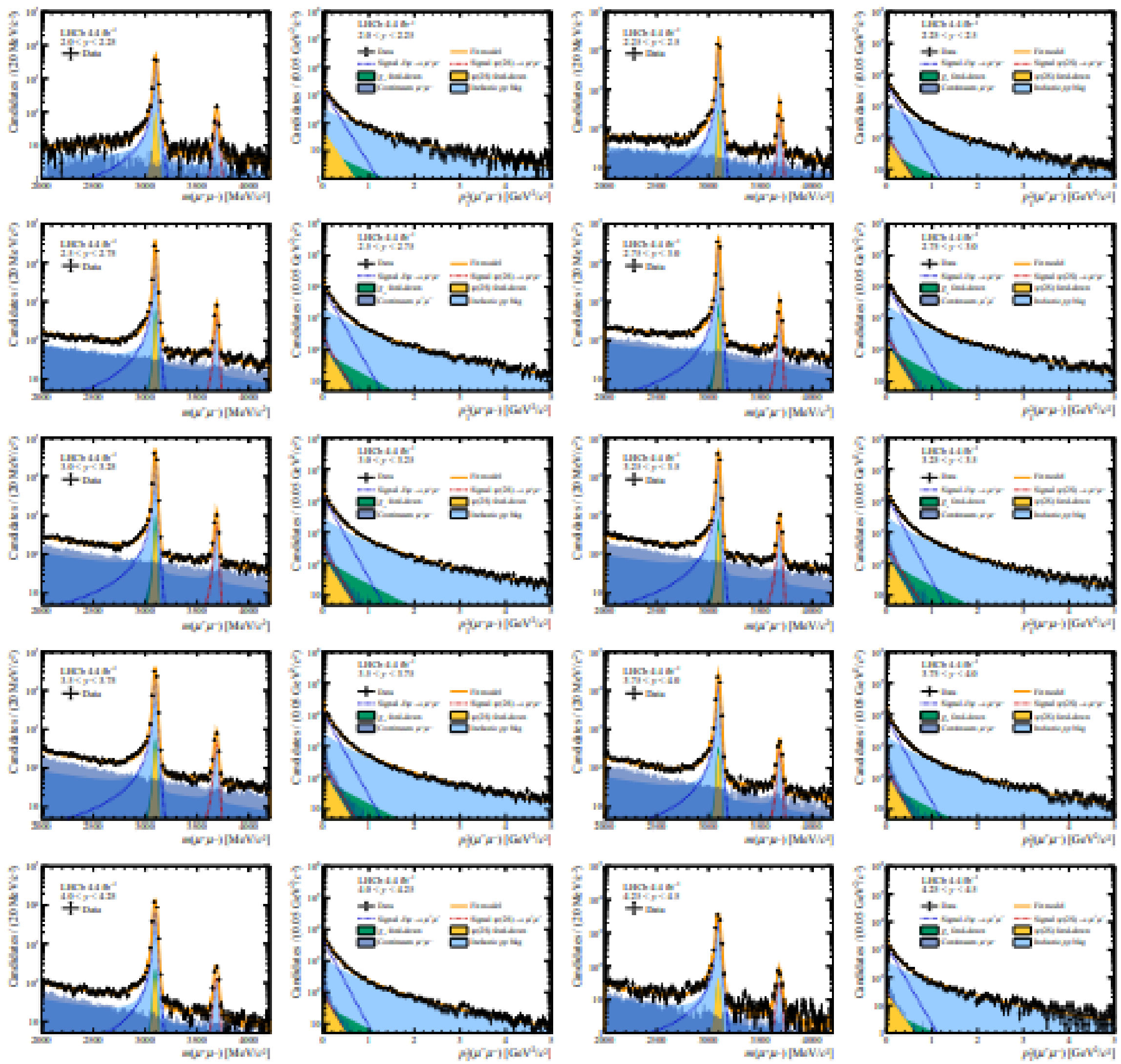

Ambiguities of Photon Emitter

The outgoing protons are not detected at LHCb!

$$\frac{\mathrm{d}\sigma}{\mathrm{d}y}(pp \to p\psi p) = S^2(W_{\gamma p,+}) \left(k_+ \frac{\mathrm{d}n}{\mathrm{d}k_+}\right) \sigma_{\gamma p \to \psi p}^{W_{\gamma p,+}} + S^2(W_{\gamma p,-}) \left(k_- \frac{\mathrm{d}n}{\mathrm{d}k_-}\right) \sigma_{\gamma p \to \psi p}^{W_{\gamma p,-}}, \quad (3)$$

with $W_{\gamma p,\pm} = \sqrt{M_\psi c^2 \sqrt{s} e^{\pm|y|}}$. The $S^2(W_{\gamma p,\pm})$ terms, the so-called survival factors, are taken from Ref. [102]. The photon flux $\mathrm{d}n/\mathrm{d}k_\pm$ for photons with energy equal to $k_\pm = (M_\psi c^2/2)e^{\pm|y|}$ is calculated following Refs. [103, 104]. The photoproduction cross-sections are given by $\sigma_{\gamma p \to \psi p}^{W_{\gamma p,\pm}}$. The antiparallel γp cross-section, $\sigma_{\gamma p \to \psi p}^{W_{\gamma p,-}}$, corresponds to large values of x, as $x \sim M_\psi c^2/\sqrt{s}\, e^{-y}$ [45]. The contribution of this term to Eq. 3 is therefore expected to be small and can be constrained from theoretical predictions. The antiparallel solution is taken from the J/ψ and $\psi(2S)$ NLO cross-section predictions from Refs. [45, 94] and subtracted. Figure 10 shows the measured photoproduction cross-section

Rapidity Distributions

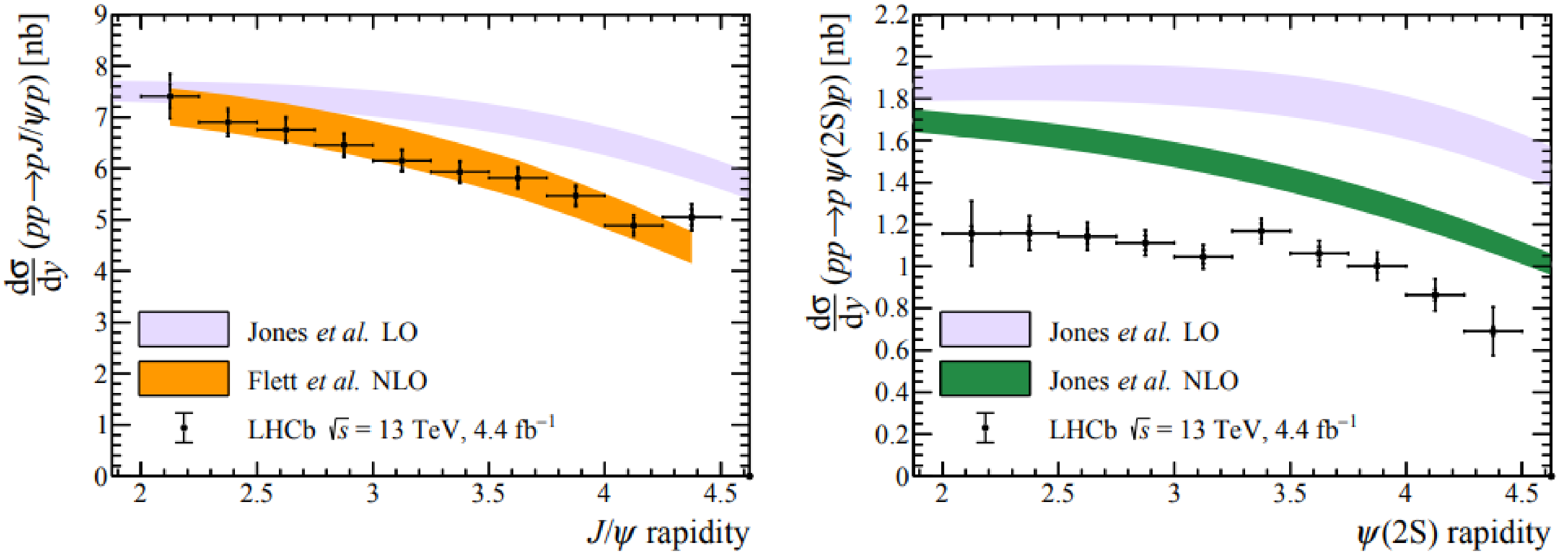

NLO calculations:
C. A. Flett, A. D. Martin, M. G. Ryskin, and T. Teubner, Very low x gluon density determined by LHCb exclusive J/ψ data, Phys. Rev. D102 (2020) 114021, arXiv:2006.13857.

psi'/Jpsi Ratios

Small rapidity dependence

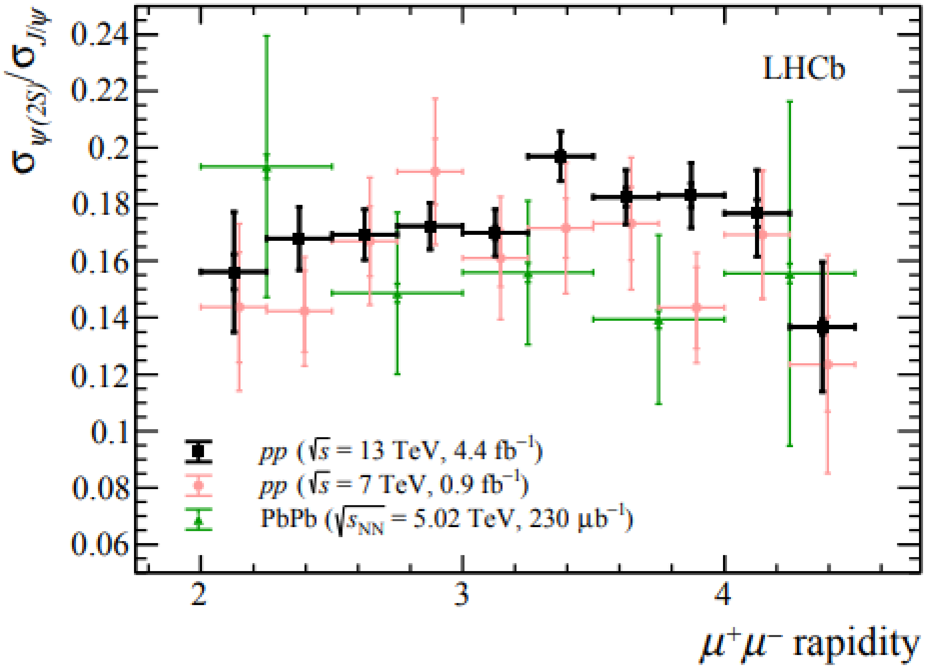

$$\frac{\sigma_{\psi(2S)}}{\sigma_{J/\psi}} = 0.1763 \pm 0.0029 \pm 0.0008 \pm 0.0039$$

Kinematic Coverage

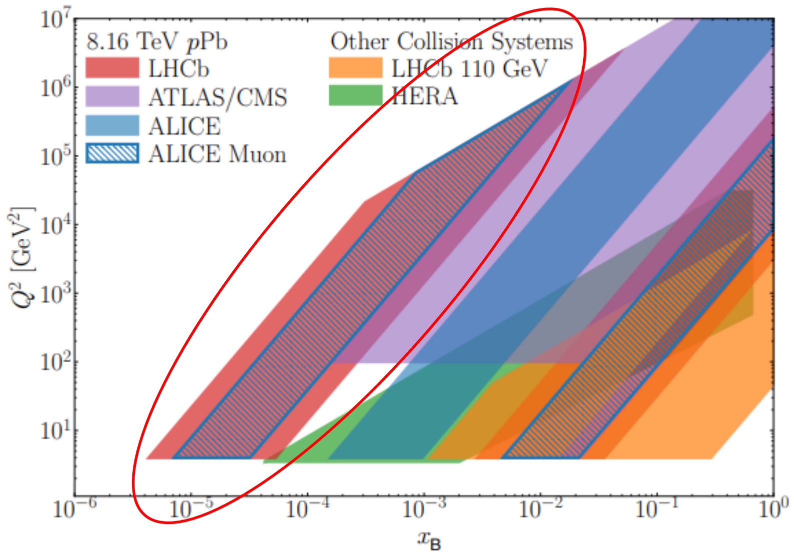

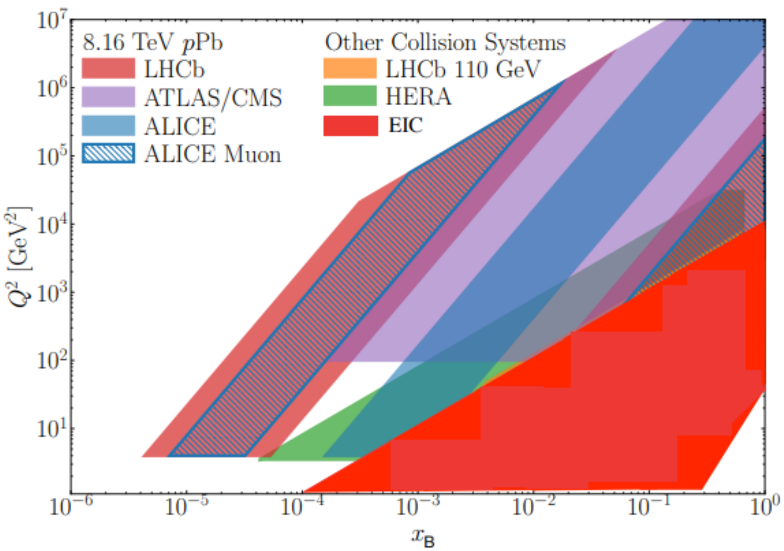

https://indico.ijclab.in2p3.fr/event/10641/contributions/35283/attachments/24301/35362/HadPhys30_2024.pdf

Theoretical Interpretation: GPDs Scheme

Exclusive processes

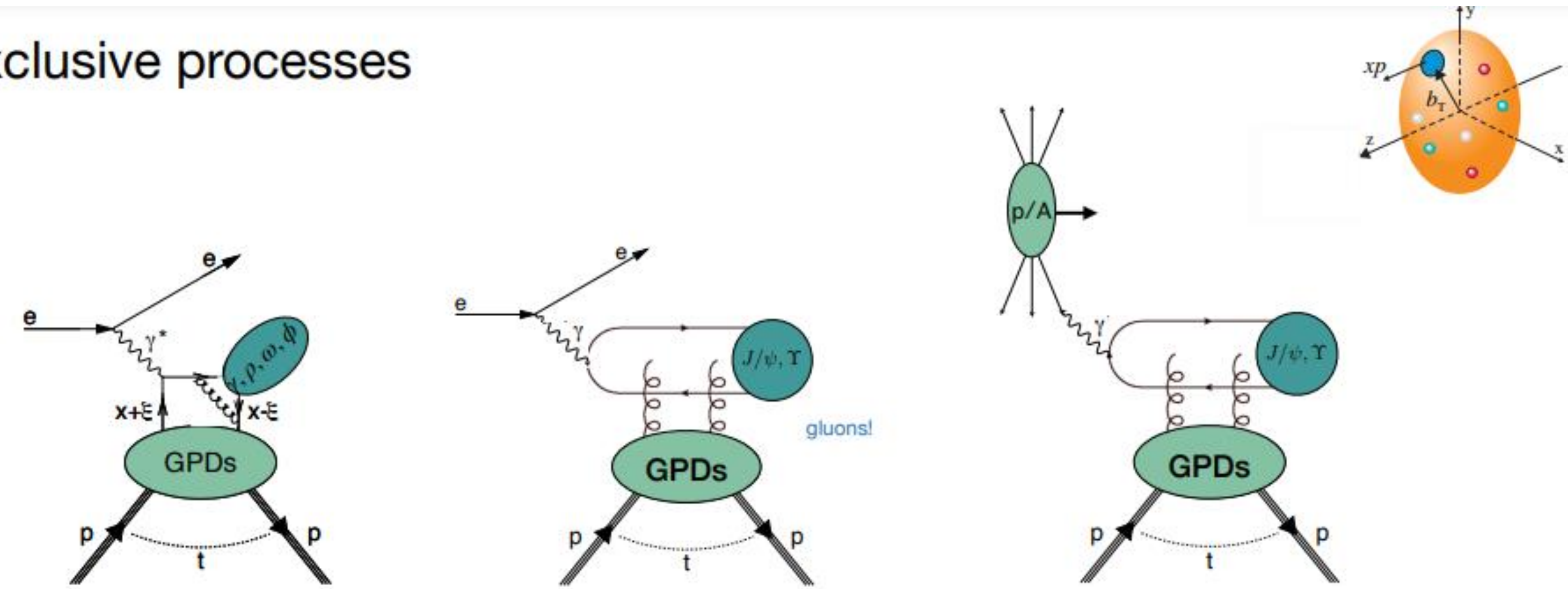

Hard exclusive meson production
Hard scale=large Q^2

Exclusive meson photoproduction
Hard scale = large charm/bottom-quark mass

Exclusive meson photoproduction
Hard scale = large charm/bottom-quark mass

down to $x_B=10^{-4}$ at HERA/EIC in ep
$x_B=10^{-3}$ at EIC in eA

down to $x_B=10^{-6}$ at LHC in pp
$x_B=10^{-5}$ at LHC in pA

Jpsi Photoproduction Cross Sections

$$x = \frac{M_{Jpsi}}{\sqrt{s}} e^{-y}$$

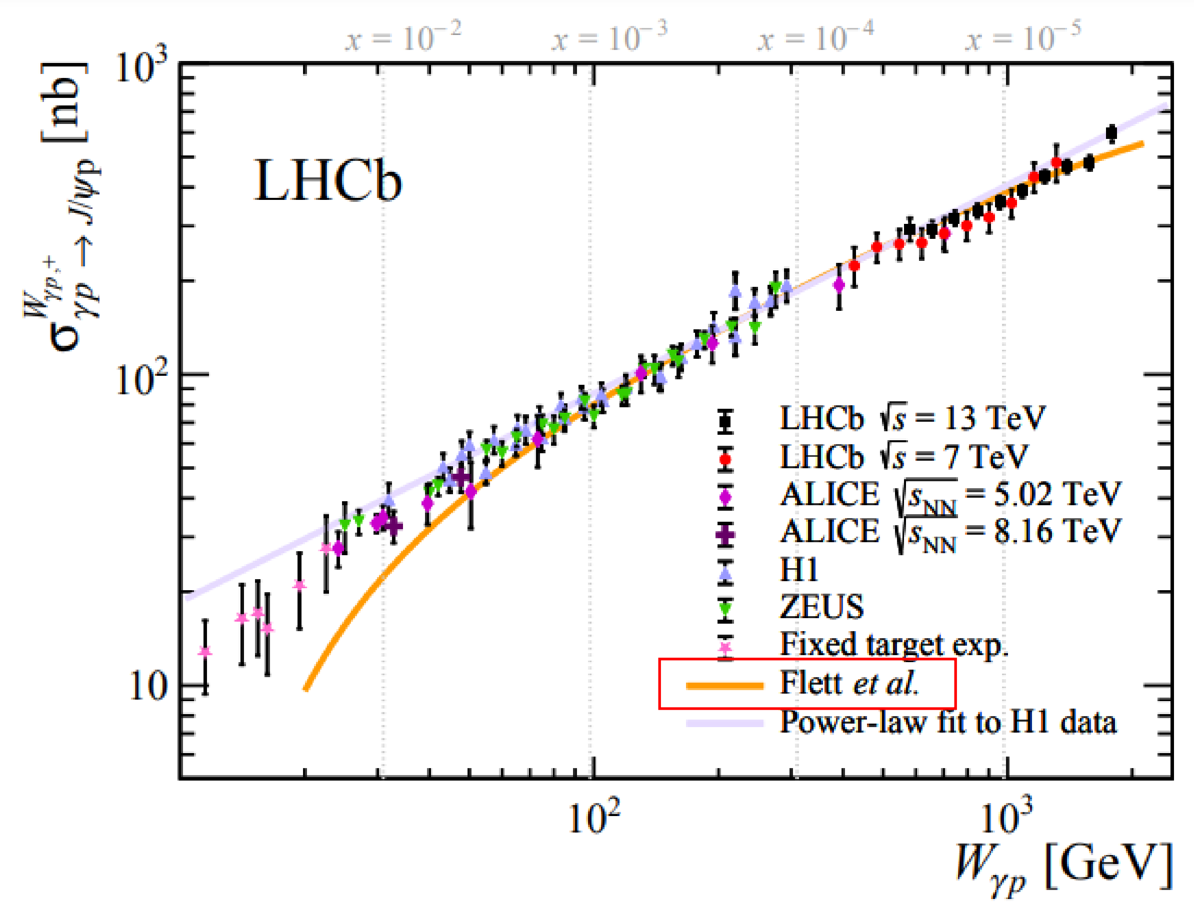

Amplitude with Collinear Factorization

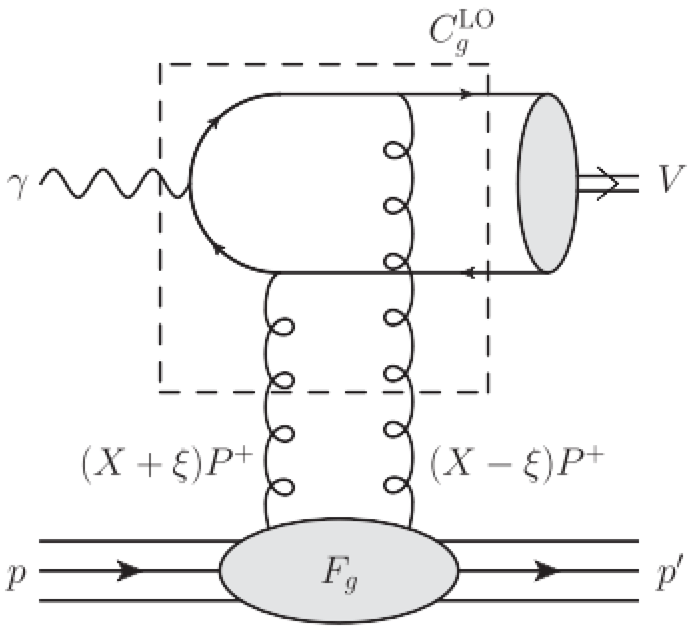

Gluon GPDs

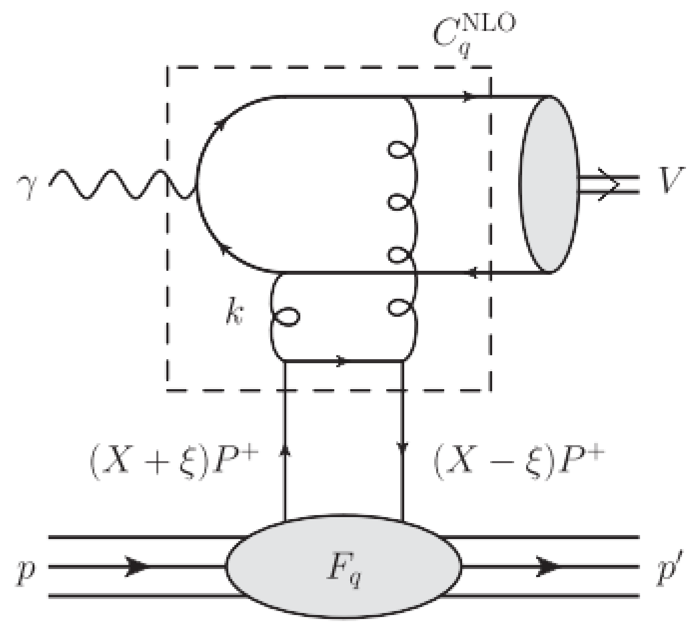

Guark singlet GPDs

$$A = \frac{4\pi\sqrt{4\pi\alpha}e_q(\epsilon_V^* \cdot \epsilon_\gamma)}{N_c}\left(\frac{\langle O_1\rangle_V}{m_c^3}\right)^{1/2} \times \int_{-1}^{1}\frac{\mathrm{d}X}{X}[C_g(X,\xi)F_g(X,\xi) + C_q(X,\xi)F_q(X,\xi)], \quad (1)$$

$\langle O_1\rangle_V$:NRQCD LDME, ccbar->Jpsi

F_q and F_g :quark singlet and gluon GPDs

“Shuvaev transform” connecting Gluon PDFs and GPDs

The Shuvaev transform, that relates the GPD to the conventional collinear gluon PDF, includes an integral over the whole x < 1 interval.

$$\mathcal{H}_q(x,\xi) = \int_{-1}^{1} \mathrm{d}x' \left[\frac{2}{\pi}\mathrm{Im}\int_0^1 \frac{\mathrm{d}s}{y(s)\sqrt{1-y(s)x'}}\right] \frac{\mathrm{d}}{\mathrm{d}x'}\left(\frac{q(x')}{|x'|}\right),$$

$$\mathcal{H}_g(x,\xi) = \int_{-1}^{1} \mathrm{d}x' \left[\frac{2}{\pi}\mathrm{Im}\int_0^1 \frac{\mathrm{d}s(x+\xi(1-2s))}{y(s)\sqrt{1-y(s)x'}}\right] \frac{\mathrm{d}}{\mathrm{d}x'}\left(\frac{g(x')}{|x'|}\right),$$

$$y(s) = \frac{4s(1-s)}{x+\xi(1-2s)}.$$

[Shuvaev et. al 1999]

$$xg(x,\mu_0^2) = Cxg^{\mathrm{global}}(x,\mu_0^2) + (1-C)xg^{\mathrm{new}}(x,\mu_0^2) \quad (4)$$

$$\text{with} \quad C = \frac{x^2}{x^2+x_0^2}, \quad (5)$$

and where xg^{global} is the value of the gluon PDF obtained in a global PDF analysis. The simplest low x form for the gluon would be

$$xg^{\mathrm{new}}(x,\mu_0^2) = nN_0(1-x)x^{-\lambda}, \quad (6)$$

where the normalization factor N_0 is chosen so that for $n=1$ the gluon PDF has the matching at $x=x_0$,

$$x_0 g^{\mathrm{new}}(x_0,\mu_0^2) = x_0 g^{\mathrm{global}}(x_0,\mu_0^2). \quad (7)$$

Matching point, $x_0 = 10^{-3}$

Gluon GPDs (Proton PDFs) vs. Data

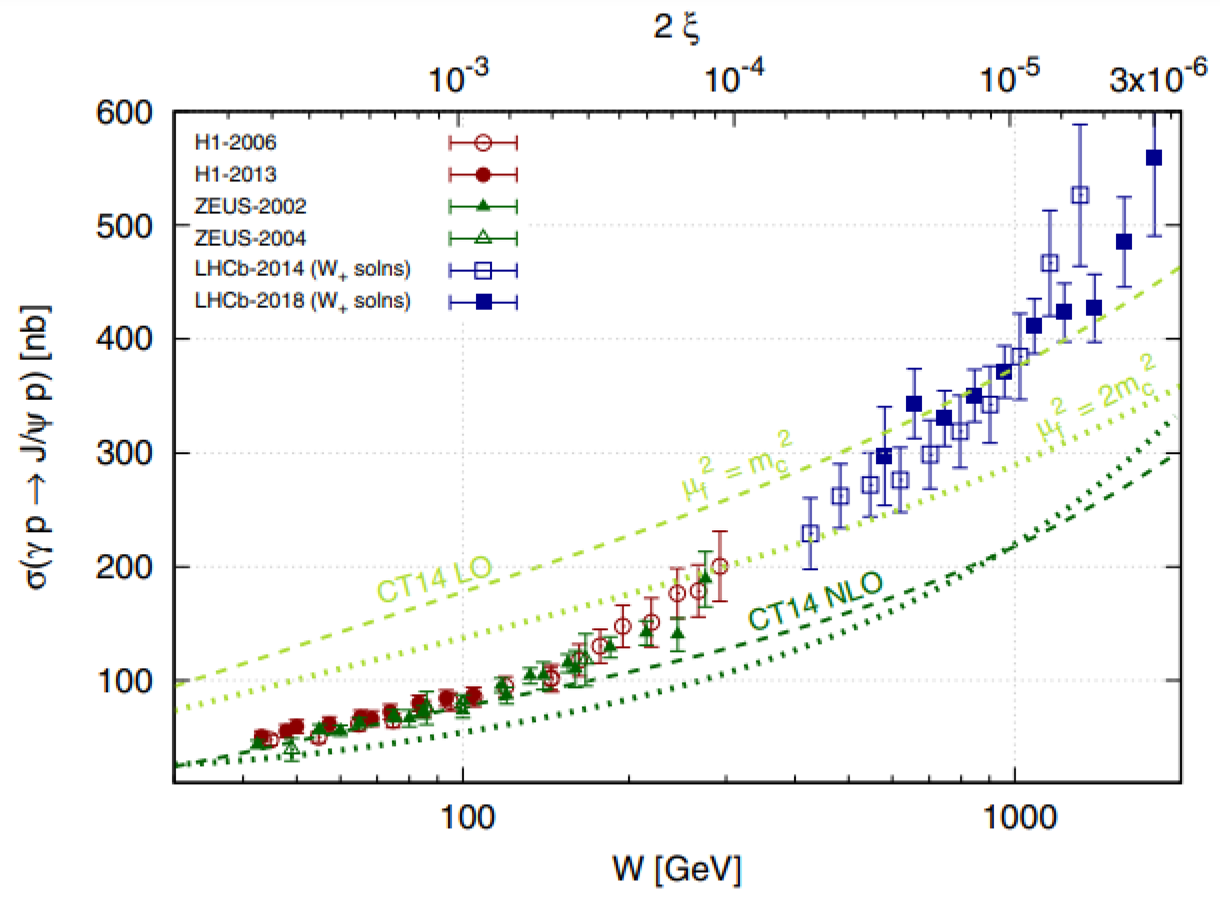

Good agreement with H1, ZEUS (x>10-4), but not LHCb (x<10-4)

Gluon GPDs (Proton PDFs, Parametrized Gluon PDFs) vs. Data

$$xg^{\text{new}}(x, \mu_0^2) = nN_0(1-x)x^{-\lambda}$$

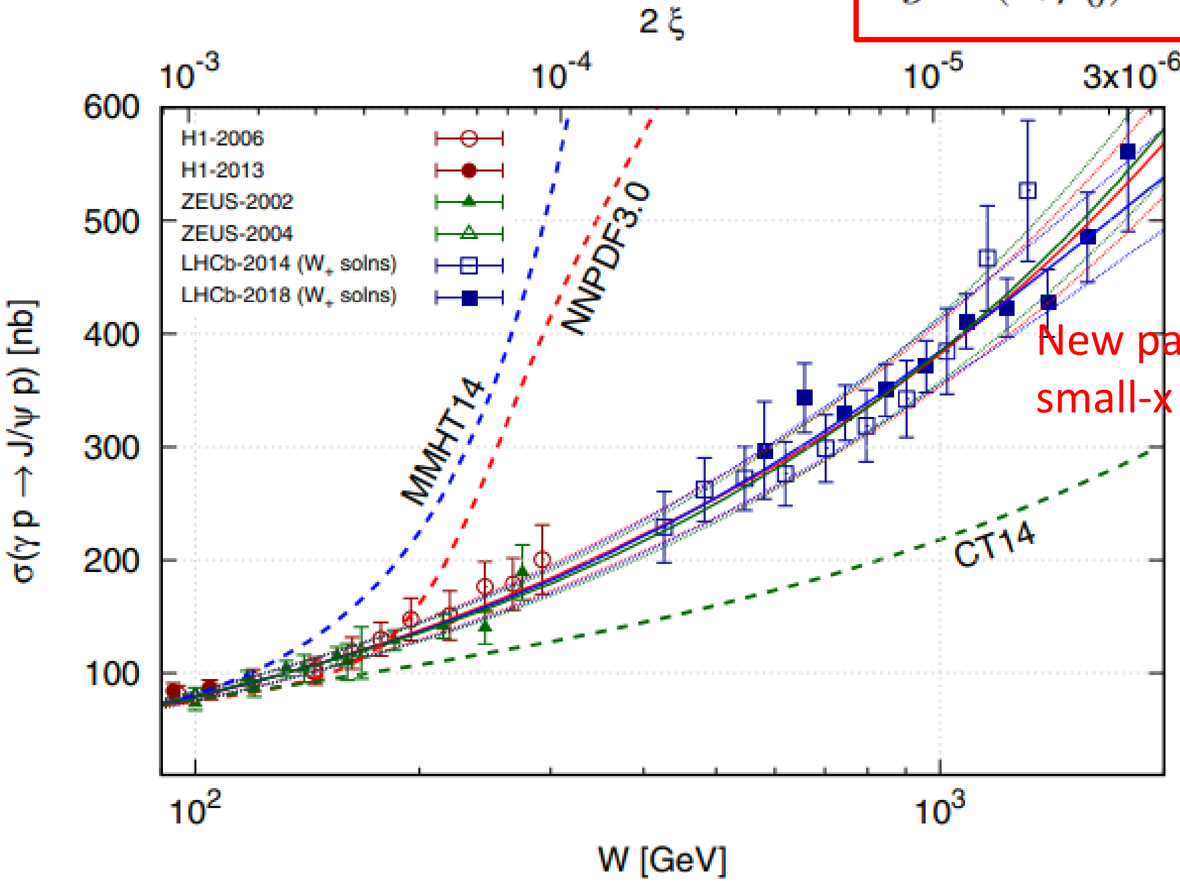

New parametrization of small-x Gluon PDFs

Good agreement with H1, ZEUS and LHCb data with new parametrization of xg.

No hint of onset of Gluon Density Saturation

$$xg^{\text{new}}(x, \mu_0^2) = nN_0(1 - x)x^{-\lambda}$$

TABLE I. The values of λ and n obtained from fits to the J/ψ data using three sets of global partons. The respective values of the total χ^2_{min} (and χ^2_{min}/d.o.f) for 45 data points are also shown.

	λ	n	χ^2_{min}	χ^2_{min}/d.o.f
NNPDF3.0	0.136	0.966	44.51	1.04
MMHT14	0.136	1.082	47.00	1.09
CT14	0.132	0.946	48.25	1.12

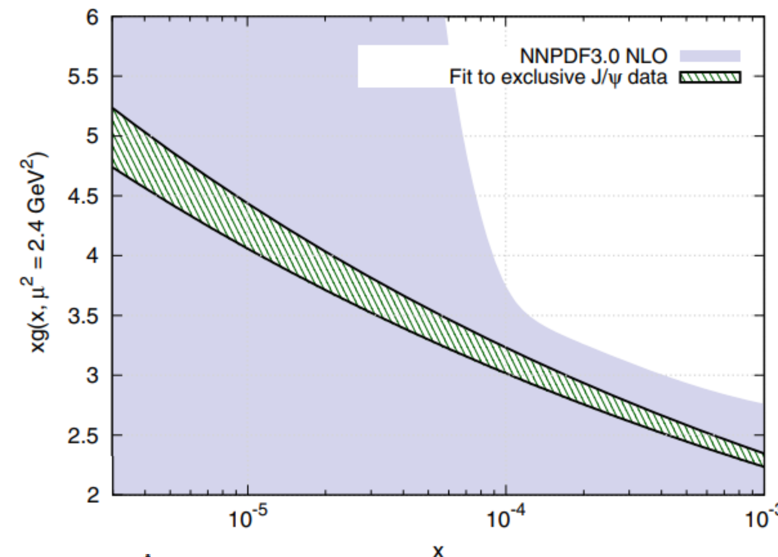

corrections rather than *saturation*. Indeed, saturation means that the gluon density tends to a constant value, $xg(x, \mu^2) \to$ const as $x \to 0$ and at a fixed scale μ [30]. That is, the power λ in (6) behaves as $\lambda \to 0$. A first hint of saturation would be to observe that the power λ (measured in some small-x interval) starts to decrease with decreasing x. The data, as shown in Fig. 3, do not indicate such behavior.

$$x \sim 10^{-5} \text{ and } \mu^2 = 2.4 \text{ GeV}^2$$

Summary

- At LHC, Ultra-Peripheral Collisions (UPC) are interesting processes to study for the physics related to EIC: nuclear/nucleon parton density, small-x gluon saturation…
- LHCb has measured the photoproduction of Jpsi at large W, which could be sensitive to the small-x gluon density of protons.
- Theoretical study which involves the proton GPD in Jpsi photoproduction shows no evident of gluon saturation down to $x=3\times10^{-6}$.